Vehicle Positioning Utilizing Single-Snapshot DOA and Signal Magnitude-Phase Estimation

Ye Tian, *Member, IEEE*, Shiqi Shu, Wei Liu, *Senior Member, IEEE*,
He Xu, and Hua Chen, *Senior Member, IEEE*

***Abstract*—Most of existing direction of arrival (DOA) based vehicle positioning techniques are established on array sample covariance matrix and multiple measurement data, which suffer from severe performance degradation in case of a single snapshot. In this paper, a challenging vehicle positioning scheme based on single-snapshot DOA and impinging signal magnitude-phase estimation is proposed. In detail, DOA is initially estimated by applying the generalized approximate message passing combined with belief propagation (GAMP-BP) algorithm under the assumption of complex discrete random variable with distinct phase information. Depending on the initial DOA estimates, two efficient approaches are respectively investigated for final DOA and signal magnitude-phase estimation, where the refine-grid GAMP combined with the least squares algorithm (GAMP-LS) and the special reweighted sparse total least-squares (SRE-STLS) are respectively adopted. With available DOA and magnitude-phase estimates, a principle for selecting reliable DOA sets is further designed, finally enabling improved vehicle positioning without ambiguity under multiple collaborative road side units (RSUs). Simulations are performed to show the effectiveness of the proposed solution.**

***Index Terms*—Vehicle positioning, DOA estimation, magnitude-phase estimation, GAMP, least squares, reweighted STLS.**

I. Introduction

With rapid development of the automotive industry, high-precision positioning technology is becoming more and more important, which not only facilitates the tracking and path planning of autonomous vehicles, but also holds significance for realizing various location sharing based network connections [1], [2], [3]. Although the global positioning system (GPS) enabled positioning technology can provide good support in most application scenarios, it is not always available anywhere, due to occlusion issues caused by tunnels and clouds. Moreover, in urban areas with dense building, GPS signals can be easily affected by interference and blocking. As a result, its positioning accuracy can be reduced to only 10 or 20 m [4]. Under such circumstances, developing wireless positioning solutions based on cooperative base stations (BSs) and road side units (RSUs) will have significant value and enormous potential commercial prospects [5], [6].

There are mainly four different types of wireless cooperative positioning approaches, which are respectively built on the received signal strength (RSS) [7], time of arrival (TOA) [8], time difference of arrival (TDOA) [9] and direction of arrival (DOA) [10], [11]. Accurate estimation by the RSS based approach relies on *prior* knowledge of the channel state information (CSI) and/or channel fading characteristics, which is normally difficult to obtain accurately. The TOA and TDOA based approaches require perfect synchronization of clocks between all nodes, which is still difficult to achieve in practice. In contrast, the DOA based solution can make full use of array aperture, requires neither *prior* CSI, nor accurate clock synchronization, making it one of the most competitive solutions [12].

Till now, several DOA based vehicle positioning methods have been investigated. In [12], a vehicle positioning scheme depending on vehicular *ad hoc* networks (VANETs) and robust DOA estimation was proposed, where the perturbed multiple signal classification (MUSIC) algorithm was adopted to achieve DOA estimation in the presence of mutual coupling. In [13], a vibrio foraging optimization (VFO) based vehicle positioning strategy aided by multiple reconfigurable intelligent surfaces (RISs) was introduced. Different from [12], closed-form DOA estimation was achieved via matrix reconstructed estimation of signal parameters by rotational invariance technique (MR-ESPRIT), yielding a low-complexity solution. These two methods are good attempts for vehicle positioning from a statistical information processing perspective. However, this type of methods not only requires a sufficient number of snapshots to obtain robust covariance matrix and eigenvector estimates, but also suffers from the serious signal-to-noise ratio (SNR) threshold effect. In other words, they are very sensitive to the number of snapshots and the SNR [14], [15], limiting their applications in certain scenarios. To tackle these problems, the sparse signal reconstruction (SSR) enabled solutions were introduced in recent years. In [16] and [17], two collaborative vehicle positioning approaches utilizing sparse Bayesian learning (SBL) and block SBL based DOA estimation were presented. With their robustness to noise and direct applications of the time-domain array output data, they maintain superior performance in both DOA estimation and vehicle positioning under a low SNR and/or with a small number of snapshots. Nevertheless, the SBL-based algorithms normally require the inverse operation of high-dimensional matrices, so their real-time responsiveness needs further improvement. As another

This work was supported by the Natural Science Foundation of Ningbo Municipality under Grant 2024J232, the Zhejiang Provincial Natural Science Foundation of China under Grant LY23F010004, and the Hong Kong Polytechnic University start-up fund with project ID P0053642. (*Corresponding Author: Wei Liu*).

Ye Tian, Shiqi Shu and Hua Chen are with the the Faculty of Electrical Engineering and Computer Science, Ningbo University, Ningbo 315211, China (e-mail: tianfield@126.com; kfhg6h@163.com; dkchenhua0714@hotmail.com). Wei Liu is with the Department of Electrical and Electronic Engineering, Hong Kong Polytechnic University, Kowloon, Hong Kong (e-mail: wei2.liu@polyu.edu.hk). He Xu is with the School of Cyber Science and Engineering, Ningbo University of Technology, Ningbo 315211, China (e-mail: xuhebest@sina.com).

alternative, the deep learning (DL) based scheme was proposed to cope with the problem of DOA based vehicle positioning. In [18], the SBLNet under the conformal array configuration was adopted for super-resolution DOA estimation of autonomous vehicles, and in [19], vehicle positioning with the dual one-dimensional convolutional neural network (D1D-CNN) based DOA estimation was proposed, which shows improved performance under multipath transmission and array uncertainties. The main problem of DL based solutions lie in the need for a large amount of data for network training, which may not be easily available in practice.

In this paper, we introduce a new vehicle positioning method with only one single snapshot from the SSR perspective in a cooperative manner, where a two-stage multiple parameters estimation based strategy from each RSU is exploited. At the first stage, DOA estimation is obtained by applying the general approximate message passing (GAMP) [20] algorithm, which has been demonstrated to better balance estimation accuracy and computational complexity than the SBL algorithm [21]. With available initial DOA estimates, improved DOA estimation result, as well as subsequent magnitude and phase information of impinging source signals are obtained by the designed two efficient strategies at the second stage. According to the estimated multi-parameters, a proper principle for selecting reliable DOA sets, as well as achieving robust vehicle positioning without ambiguity is finally developed. The main contributions of this work are as follows:

- The GAMP combined with belief propagation (GAMP-BP) is used for initial DOA estimation under the assumption of complex discrete random variable with distinct phase information, which provides a solid foundation for subsequent real-time vehicle positioning, as well as a potential way to avoid ambiguity in vehicle positioning.
- Two enhanced DOA and magnitude-phase estimation approaches, respectively relying on the refine-grid GAMP combined with least squares (GAMP-LS) and the special reweighted sparse total least-squares (SRE-STLS) algorithms, are developed with a single snapshot, which provide satisfactory multi-parameter estimation results, with trade-off between estimation accuracy and complexity; such a feature is of great significance for subsequent high-performance vehicle positioning.
- A novel vehicle positioning mechanism established on the DOA and magnitude-phase estimation results is designed, which provides a simple and feasible way for reliable positioning without requiring identity labels. To the best of our knowledge, it is the first time to explore multi-parameter estimation result to enhance the vehicle positioning performance. Extensive simulations in various array configurations are performed, which demonstrates that the proposed solutions can not only yield satisfactory and computationally efficient multi-parameter estimation results, but also lead to a significantly improved positioning performance by further utilizing the designed positioning mechanism.

Notations: Upper-case (lower-case) boldface letters denote matrices (vectors). The superscripts $(\cdot)^T$, $(\cdot)^H$ and $(\cdot)^{-1}$ represent the transpose, conjugate transpose and inverse operations, respectively. $\mathrm{diag}\{\cdot\}$ denotes the diagonalization operation and $\mathrm{tr}(\cdot)$ the trace of a matrix. $\|\cdot\|_F$, $\|\cdot\|_2$ and $\|\cdot\|_1$ stand for the Frobenius norm, ℓ_2 norm and ℓ_1 norm, respectively. $\mathbf{x} \sim \mathcal{CN}(\boldsymbol{\mu}, \boldsymbol{\Sigma})$ means that $\mathbf{x}$ follows a complex Gaussian distribution with mean $\boldsymbol{\mu}$ and covariance $\boldsymbol{\Sigma}$. $|\cdot|$ and $\angle[\cdot]$ denote the absolute value and phase of a complex number, respectively. $\mathbf{I}_M$ is the $M \times M$ identity matrix, $\mathbf{0}_M$ the $M \times M$ all-zero matrix and $\delta(\cdot)$ the Dirac delta function.

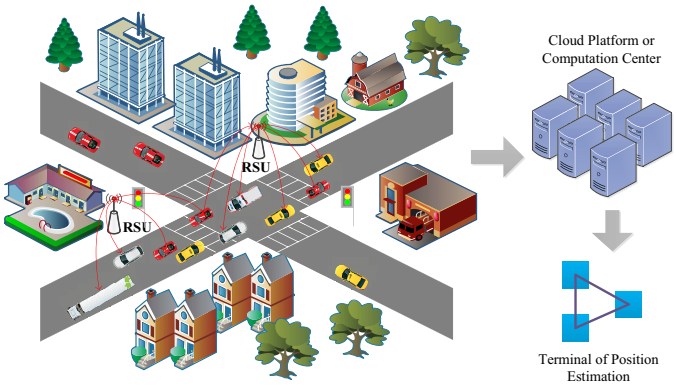

Fig. 1. Schematic diagram for the considered vehicle positioning system.

The paper is organized as follows. The positioning system and data model are introduced in Section II. The proposed DOA and magnitude-phase estimation algorithm is detailed in Section III. The vehicle positioning scheme utilizing DOA and magnitude-phase estimation result is presented in Section IV. Simulation results are provided in Section V, and conclusions are drawn in Section VI.

II. Positioning System and Data Model

The considered vehicle positioning system is shown in Fig. 1, which consists of three key modules: 1) vehicle terminals, each equipped with a single antenna to transmit positioning signal with different phase information; 2) multiple RSUs, each equipped with an M-element uniform linear array (ULA) with inter-sensor element spacing $d = \lambda/2$, responsible for receiving positioning signals from vehicle terminals, where λ is the carrier wavelength; 3) cloud platform and/or computation center, which are mainly used to perform DOA and incident signal magnitude-phase estimation by suitable signal processing algorithms, and further provide unambiguous positions of vehicles with available DOA and magnitude-phase information.

The key for the considered vehicle positioning architecture is how to achieve satisfactory and computationally efficient DOA and magnitude-phase estimation of the positioning signals. Although there have been many high-precision DOA estimation algorithms, efficient algorithms capable of simultaneously estimating both DOA and magnitude-phase information are still scarce. Under such circumstances, we first develop a suitable single-snapshot DOA and signal magnitude-phase estimation algorithm from the SSR perspective, and then

achieve vehicle positioning in a collaborative way through multiple RSUs.

The signal model of DOA and magnitude-phase estimation at a certain RSU under the assumption of K incident signals can be formulated as

$$\mathbf{y} = \mathbf{A}\boldsymbol{\beta} + \mathbf{n} = \sum_{k=1}^{K} \mathbf{a}\left(\theta_k\right)\beta_k + \mathbf{n} \tag{1}$$

where the array output $\mathbf{y} \in \mathbb{C}^{M\times 1}$, received signal vector $\boldsymbol{\beta} \in \mathbb{C}^{K\times 1}$, independent and identically distributed additive white noise vector $\mathbf{n} \in \mathbb{C}^{M\times 1}$ with variance $\sigma_n^2\mathbf{I}$, array steering matrix $\mathbf{A} \in \mathbb{C}^{M\times K}$ and its k-th column $\mathbf{a}\left(\theta_k\right) \in \mathbb{C}^{M\times 1}$ are respectively given by

$$\begin{aligned}
\mathbf{y} &= \left[y_1, y_2, \ldots, y_M\right]^T \\
\boldsymbol{\beta} &= \left[\beta_1, \beta_2, \ldots, \beta_K\right]^T \\
\mathbf{n} &= \left[n_1, n_2, \ldots, n_M\right]^T \\
\mathbf{A} &= \left[\mathbf{a}\left(\theta_1\right), \mathbf{a}\left(\theta_2\right), \ldots, \mathbf{a}\left(\theta_K\right)\right] \\
\mathbf{a}\left(\theta_k\right) &= \left[1, e^{-j\pi\sin\theta_k}, \ldots, e^{-j\pi(M-1)\sin\theta_k}\right]^T
\end{aligned}$$

where $\beta_k = \rho_k e^{j\phi_k}$ with ρ_k and ϕ_k representing the magnitude and phase of the k-th incident signal.

Let $\boldsymbol{\Phi} \in \mathbb{C}^{M\times N}$ denote the overcomplete basis matrix (OBM) of $\mathbf{A}$, which corresponds to the N-sample grid of all potential DOAs $\{\bar{\theta}_1, \bar{\theta}_2, \ldots, \bar{\theta}_N\}$ in the spatial domain with $N \gg K$. Consequently, $\mathbf{y}$ can be rewritten as

$$\mathbf{y} = \boldsymbol{\Phi}\mathbf{x} + \mathbf{n} \tag{2}$$

where $\mathbf{x}$ is a K-sparse vector, whose g-th element is non-zero and equals β_k if the signal emitted from the k-th vehicle comes from $\bar{\theta}_g$ and zeros otherwise.

Note that the signals $\boldsymbol{\beta}$ in our considered scenario need to contain different phase information, which will be used to distinguish different vehicles at the RUS sides. Therefore, it is further assumed here that x_j is controlled by a binary variable $s_j \in \{0, 1\}$, where $s_j = 1$ implies that x_j is a nonzero discrete random variable that follows a uniform distribution, with a sample space of $\{u_1, \ldots u_E\}$ (E stands for the cardinality of the sample space), $s_j = 0$ indicates that $x_j = 0$, and $p\left(s_j = 1\right) = \lambda_j$, $p\left(s_j = 0\right) = 1 - \lambda_j$. Consequently, the probability density function (PDF) of the j-th element x_j of $\mathbf{x}\left(t\right)$ can be expressed as

$$p(x_j) = (1-\lambda_j)\delta\left(x_j\right) + \lambda_j \sum_{e=1}^{E} p_e \delta\left(x_j - u_e\right) \tag{3}$$

where $p_e = 1/E$. In the following, we first demonstrate how to exploit $\mathbf{y}$, $\boldsymbol{\Phi}$ and its refined value to achieve accurate DOA and signal magnitude-phase estimation, and then propose the robust collaborative vehicle positioning scheme by jointly utilizing the estimated information.

III. Proposed Method

In this section, we first present the method for accurate and computationally efficient DOA and signal magnitude-phase estimation, and then combine them to achieve robust collaborative vehicle positioning without ambiguity.

TABLE I
DISTRIBUTION AND FUNCTIONAL FORM OF EACH FACTOR

Factor	Distribution	Functional Form
$g_i(\mathbf{x})$	$p\left(y_i\middle\|\mathbf{x}\right)$	$\mathcal{CN}\left(y_i; \mathbf{a}_i^T\mathbf{x}, \sigma_0^2\right)$
$f_j(x_j, s_j)$	$p\left(x_j\middle\|s_j\right)$	$\sum_{e=1}^{E} p_e\delta\left(x_j - s_j u_e\right)$
$h_j(s_j)$	$p\left(s_j\right)$	$\left(1-\lambda_j\right)^{1-s_j}\lambda_j{}^{s_j}$

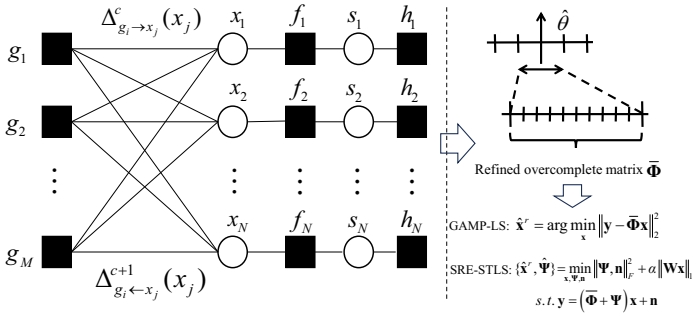

Fig. 2. Framework of the proposed method, where the left part is adopted for initial DOA estimation, and the right part for improved DOA and incident signal magnitude-phase estimation.

A. Initial DOA Estimation with GAMP-BP

Considering the real-time response requirement of vehicle positioning in practice, the computationally efficient GAMP algorithm is adopted for initial DOA estimation, which is derived from the loopy belief propagation algorithm (LBPA) designed for the bipartite graph model [20]. The LBPA is able to produce the posterior distribution within a few iterations and consequently the minimum mean-squared error (MMSE) estimates of $\mathbf{x}$. Meanwhile, we also apply the belief propagation (BP) [22] algorithm to reconstruct $\mathbf{s}$. The joint posterior PDF of $\mathbf{x}$ and $\mathbf{s}$ for a given $\mathbf{y}$ can be expressed as

$$p\left(\mathbf{x}, \mathbf{s}\middle|\mathbf{y}\right) \propto \prod_{i=1}^{M} p\left(y_i\middle|\mathbf{x}\right) \prod_{j=1}^{N} p\left(x_j\middle|s_j\right) \prod_{j=1}^{N} p\left(s_j\right) \tag{4}$$

whose factor graph is illustrated in the left part of Fig. 2, and the functional form of each factor is given in Table I, where $\mathbf{a}_i$ is an abbreviation of $\mathbf{a}\left(\theta_i\right)$, representing the steering vector corresponding to the DOA θ_i, $i = 1, \ldots, N$.

For the considered model, the message passing process can be divided into three steps. The first step is to calculate the following three messages between factor nodes and variable nodes, respectively expressed at the l-th iteration as

$$\Delta^{l}_{s_j\to f_j}(s_j) = \Delta^{l}_{h_j\to s_j}(s_j) = \left(1-\lambda_j^{l-1}\right)^{1-s_j}\left(\lambda_j^{l-1}\right)^{s_j} \tag{5}$$

$$\begin{aligned}
\Delta^{l}_{f_j\to x_j}(x_j) &= \sum_{s_j=0}^{1} \Delta^{l}_{s_j\to f_j}(s_j) f\left(x_j, s_j\right) \\
&= \left(1-\lambda_j^{l-1}\right)\delta\left(x_j\right) + \lambda_j^{l-1}\sum_{e=1}^{E} p_e\delta\left(x_j - u_e\right)
\end{aligned} \tag{6}$$

with initialized parameters $\lambda_j^{l-1} = \lambda_j^0 = 0.1$.

The second step is to estimate the posterior PDF of $\mathbf{x}$, which can be solved by the GAMP algorithm. By utilizing the message $\Delta^l_{f_j\to x_j}(x_j)$ obtained from the first step as the *prior* information for x_j, and according to the sum product algorithm (SPA) in [22], [23], the transmission of messages in factor graphs at the c-th iteration can be mainly divided into the following two categories:

$$\Delta^c_{g_i\to x_j}(x_j) = const \cdot \int_{\{x_f\}_{f\neq j}} g_i(\mathbf{x}) \prod_{f\neq j} \Delta^c_{g_i\leftarrow x_f}(x_f) \quad (7)$$

$$\Delta^{c+1}_{g_i\leftarrow x_j}(x_j) = const \cdot \Delta^l_{f_j\to x_j}(x_j) \prod_{f\neq i} \Delta^c_{g_f\to x_j}(x_j) \quad (8)$$

where $const$ is a constant greater than 0, and $\Delta^1_{g_i\leftarrow x_j}(x_j) = \Delta^l_{f_j\to x_j}(x_j)$.

Note that SPA estimates the posterior PDF of a given variable by calculating the product of messages entering that variable node (after appropriate scaling), which directly yields

$$\Delta^c_{x_j}(x_j) = const \cdot \sum_{i=1}^{M} \Delta^c_{g_i\to x_j}(x_j)\Delta^l_{f_j\to x_j}(x_j). \quad (9)$$

Through approximation according to the central limit theorem (CMT) and Taylor expansion, it can be derived that the MMSE estimate of x_j, as well as the variance of $\Delta^c_{x_j}(x_j)$, can be given by

$$\hat{x}_j(c+1) = \mathbb{E}\left\{\Delta^c_{x_j}(x_j)\right\} = g_{in}\left(c, \hat{r}_j(c), \tau^r_j(c)\right) \quad (10)$$

$$\tau^x_j(c+1) = \mathrm{Var}\left\{\Delta^c_{x_j}(x_j)\right\} = \tau^r_j \frac{\partial g_{in}\left(c, \hat{r}_j(c), \tau^r_j(c)\right)}{\partial \hat{r}_j} \quad (11)$$

where $\tau^r_j(c)$ and $\hat{r}_j(c)$ are the updated parameters related to $\hat{x}_j(c)$, $\mathbf{y}$ and elements of OBM $\mathbf{\Phi}$ [19].

By initializing the parameters

$$\hat{x}_j(c) = \hat{x}_j(1) = \int_{x_j} x_j \Delta^l_{f_j\to x_j}(x_j) \quad (12)$$

$$\tau^x_j(c) = \tau^x_j(1) = \int_{x_j} |x_j - \hat{x}_j(1)|^2 \Delta^l_{f_j\to x_j}(x_j) \quad (13)$$

at this step, g_{in} and g_{out} can be respectively given by

$$g_{in}\left(c, \hat{r}_j(c), \tau^r_j(c)\right) = \frac{\sum_{e=1}^{E} u_e p_e \mathcal{CN}\left(u_e; \hat{r}_j(c), \tau^r_j(c)\right)}{(1+\gamma)\sum_{e=1}^{E} p_e \mathcal{CN}\left(u_e; \hat{r}_j(c), \tau^r_j(c)\right)} \quad (14)$$

$$g_{out}\left(c, \hat{p}_i(c), y_i, \tau^p_i(c)\right) = \frac{y_i - \hat{p}_i(c)}{\tau_0 + \tau^p_i(c)} \quad (15)$$

whose corresponding first-order derivative can be written as

$$\tau^r_j \frac{\partial g_{in}\left(c, \hat{r}_j(c), \tau^r_j(c)\right)}{\partial \hat{r}_j} = \frac{\sum_{e}^{E} |u_e|^2 p_e \mathcal{CN}\left(u_e; \hat{r}_j(c), \tau^r_j(c)\right)}{(1+\gamma)\sum_{e}^{E} p_e \mathcal{CN}\left(u_e; \hat{r}_j(c), \tau^r_j(c)\right)} - |g_{in}|^2 \quad (16)$$

$$\frac{\partial}{\partial \hat{p}_i} g_{out}\left(c, \hat{p}_i(c), y_i, \tau^p_i(c)\right) = -\frac{1}{\tau_0 + \tau^p_i(c)} \quad (17)$$

with

$$\gamma = \frac{\left(1-\lambda^{l-1}_j\right)\mathcal{CN}\left(0; \hat{r}_j(c), \tau^r_j(c)\right)}{\lambda^{l-1}_j \sum_{e=1}^{E} p_e \mathcal{CN}\left(u_e; \hat{r}_j(c), \tau^r_j(c)\right)}. \quad (18)$$

With available parameters at the second step, and the PDF estimation of $\mathbf{x}$ obtained from GAMP, the passing messages from x_j to f_j and f_j to s_j can be calculated as

$$\Delta^l_{x_j\to f_j}(x_j) = \mathcal{CN}\left(x_j; \hat{r}_j(l), \tau^r_j(l)\right) \quad (19)$$

and

$$\Delta^l_{f_j\to s_j}(s_j) \propto \int_{x_j} f_j(x_j, s_j) \cdot \Delta^l_{x_j\to f_j}(x_j) = \sum_{e=1}^{E} p_e \mathcal{CN}\left(s_j u_e; \hat{r}_j(l), \tau^r_j(l)\right) \quad (20)$$

respectively, where $\hat{r}_j(l) = \hat{r}_j(C)$, $\tau^r_j(l) = \hat{r}_j(C)$, and C is the number of GAMP inner iterations.

After the normalization of $\Delta^l_{f_j\to s_j}(s_j)$, λ^l_j is subsequently updated to

$$\lambda^l_j = \Delta^l_{f_j\to s_j}(s_j = 1) = \frac{\sum_{e=1}^{E} p_e \mathcal{CN}\left(s_j u_e; \hat{r}(l), \tau^r_j(l)\right)}{\sum_{e=1}^{E} p_e \mathcal{CN}\left(s_j u_e; \hat{r}(l), \tau^r_j(l)\right) + \sum_{e=1}^{E} p_e \mathcal{CN}\left(0; \hat{r}(l), \tau^r_j(l)\right)}. \quad (21)$$

By updating λ, $\mathbf{x}$ and $\mathbf{s}$ alternately, we can finally obtain the estimate $\hat{\mathbf{x}}$ of $\mathbf{x}$, and then by finding its indexes of K largest values, the DOAs related to a certain RSU are obtained as $\{\tilde{\theta}_1, \ldots, \tilde{\theta}_K\}$. The initial DOA estimation process utilizing GAMP-BP is summarized in Algorithm 1, where $\Phi_{i,j}$ represents the (i,j)-th element of OBM $\mathbf{\Phi}$.

B. DOA and Magnitude-Phase Estimation with GAMP-LS

As GAMP is an approximation of LPBA, its final estimate cannot be guaranteed to be consistent [24]. On the other hand, the adopted GAMP combined with BP (i.e., GAMP-BP) algorithm is most closely related to the AMP algorithm [20], which can be regarded as an efficient implementation of the least-absolute selection and shrinkage selection operator (LASSO) [25]. However, as demonstrated in literature [26], [27], the LASSO estimator has an undemocratic penalization issue for larger coefficients, resulting in the degradation of recovery performance, especially for the signal magnitude recovery performance.

To tackle this problem, the simple and effective least-squares (LS) algorithm combined with the refine-grid GAMP (termed here as GAMP-LS) is developed in an iterative way. In detail, with DOA estimates $\{\tilde{\theta}^{\mathfrak{p}}_1, \ldots, \tilde{\theta}^{\mathfrak{p}}_K\}$ at the $\mathfrak{p}$-th iteration, a small-scale OBM $\bar{\mathbf{\Phi}} \in \mathbb{C}^{M\times \bar{N}}$ around $\{\tilde{\theta}^{\mathfrak{p}}_1, \ldots, \tilde{\theta}^{\mathfrak{p}}_K\}$ with grid interval $\check{d}$ is constructed with $\bar{N} \ll N$. Then, by performing the GAMP-BP algorithm again with OBM $\bar{\mathbf{\Phi}}$ at the $(\mathfrak{p}+1)$-th iteration, an improved DOA estimate is obtained.

Algorithm 1: Initial DOA Estimation Utilizing GAMP-BP

Input: OBM $\mathbf{\Phi}$, λ_j^0 and array output signal $\mathbf{y}$
Output: Initial DOA estimates $\{\tilde{\theta}_1, \ldots, \tilde{\theta}_K\}$
1. Initialization: for each $j = 1, 2..., N$,
$\hat{x}_j(1) = \int_{x_j} x_j p(x_j)$,
$\tau_j^x(1) = \int_{x_j} (x_j - \hat{x}_j(1))^2 p(x_j)$,
$\sigma_j^2 = \frac{\|\mathbf{y}\|_2^2 - m\sigma_e^2}{\mathrm{tr}(\mathbf{\Phi}^H\mathbf{\Phi})}$.
2. Output linear step of GAMP: for each $i = 1, 2..., M$,
$\tau_i^p(c) = \sum_j |\Phi_{ij}| \tau_j^x(c)^2$,
$\hat{p}_i(c) = \sum_j \Phi_{ij}\hat{x}_i(c) - \tau_i^p(c)\hat{s}_i(c-1)$,
where $\hat{s}_i(c-1) = 0$.
3. Output nonlinear step of GAMP: for each $i = 1, 2..., M$,
$\hat{s}_i(c) = g_{out}\left(c, \hat{p}_i(c), y_i, \tau_i^p(c)\right)$,
$\tau_i^s(c) = -\frac{\partial}{\partial \hat{p}} g_{out}\left(c, \hat{p}_i(c), y_i, \tau_i^p(c)\right)$.
4. Input linear step of GAMP: for each $j = 1, 2..., N$,
$\tau_j^r(c) = \left[\sum_i |\Phi_{ij}|^2 \tau_i^s(c)\right]^{-1}$,
$\hat{r}_j(c) = \widehat{x}_j(c) + \tau_i^r(c) \sum_i \Phi_{ij}\hat{s}_i(c)$.
5. Input nonlinear step of GAMP: for each $j = 1, 2..., N$,
$\hat{x}_j(c+1) = g_{in}\left(c, \hat{r}_j(c), \tau_j^r(c)\right)$
$\tau_j^x(c+1) = \tau_j^r(c) \frac{\partial}{\partial \hat{r}} g_{in}\left(c, \hat{r}_j(c), \tau_j^r(c)\right)$
Update $c = c + 1$ and return to step 2 until a sufficient number of iterations have been performed.
6. Determine λ_j^l according to (19)∼(21).
Update $l = l + 1$ and return to step 1 until a sufficient number of iterations have been performed.
7. Find the indexes of K largest values of estimated $\hat{\mathbf{x}}$ to determine $\{\tilde{\theta}_1, \ldots, \tilde{\theta}_K\}$.

Subsequently, with the final refined OBM $\bar{\mathbf{\Phi}}$, the incident signal magnitude and phase information can be obtained by solving the following LS problem

$$\hat{\mathbf{x}}^r = \min_{\mathbf{x}} \left\|\mathbf{y} - \bar{\mathbf{\Phi}}\mathbf{x}\right\|_2^2 \tag{22}$$

whose solution is $\hat{\mathbf{x}}^r = \left(\bar{\mathbf{\Phi}}^H\bar{\mathbf{\Phi}}\right)^{-1}\bar{\mathbf{\Phi}}^H\mathbf{y}$.

With available $\hat{\mathbf{x}}^r$, the magnitude and phase estimates of incident source signals are obtained via

$$\tilde{\rho}_k = \left|\hat{\mathbf{x}}_k^{(r)}\right|, \ \tilde{\phi}_k = \angle[\hat{\mathbf{x}}_k^{(r)}], \ k = 1, \ldots, K. \tag{23}$$

The proposed GAMP-LS based DOA and magnitude-phase estimation method is tabulated in Algorithm 2. By initializing $\bar{\mathbf{\Phi}}$ around initial DOA estimates $\{\tilde{\theta}_1, \ldots, \tilde{\theta}_K\}$ and updating $\bar{\mathbf{\Phi}}$ with grid interval $\check{d} \leftarrow \check{d}/2$, a good and efficient multi-parameter estimation result is obtained, as shown later by simulations.

C. DOA and Magnitude-Phase Estimation with SRE-STLS

It is noted that the above LS algorithm is sensitive to noise, and may even suffer from numerical instability. Meanwhile, it does not consider the influence of angle grid bias when constructing refined OBM $\bar{\mathbf{\Phi}}$ at each iteration. To promote the robustness of multi-parameter estimation against noise, instability and grid bias, a special reweighted sparse total least-squares (termed here as SRE-STLS) algorithm is proposed for improved multi-parameter estimation, with the following formulation

$$\min_{\mathbf{x},\mathbf{\Psi},\mathbf{n}} \|\mathbf{\Psi}, \mathbf{n}\|_F^2 + \alpha\|\mathbf{W}\mathbf{x}\|_1 \ s.\ t.\ \mathbf{y} = \left(\bar{\mathbf{\Phi}} + \mathbf{\Psi}\right)\mathbf{x} + \mathbf{n} \tag{24}$$

Algorithm 2: GAMP-LS Based DOA and Magnitude-Phase Estimation

Input: Initial DOA estimates $\{\tilde{\theta}_1, \ldots, \tilde{\theta}_K\}$, received signal $\mathbf{y}$, N_{max}
Output: Refined DOA estimates $\{\tilde{\theta}_1^r, \ldots, \tilde{\theta}_K^r\}$, signal magnitude estimates $\{\tilde{\rho}_1, \ldots, \tilde{\rho}_K\}$ and signal phase estimates $\{\tilde{\phi}_1, \ldots, \tilde{\phi}_K\}$
1. Construct a small-scale OBM $\bar{\mathbf{\Phi}}$ around $\{\tilde{\theta}_1, \ldots, \tilde{\theta}_K\}$ with interval $\check{d}$.
2. **for** $i = 1 : N_{max}$
Perform **Algorithm 1** with $\bar{\mathbf{\Phi}}$ to obtain improved DOAs,
$\check{d} \leftarrow \check{d}/2$, and refine $\bar{\mathbf{\Phi}}$ around improved DOAs with interval $\check{d}$.
end
3. Output the final refined DOA estimates $\{\tilde{\theta}_1^r, \ldots, \tilde{\theta}_K^r\}$.
4. Update $\hat{\mathbf{x}}$ by solving the LS problem: $\hat{\mathbf{x}}^r = \min_{\mathbf{x}} \left\|\mathbf{y} - \bar{\mathbf{\Phi}}\mathbf{x}\right\|_2^2$
i.e., $\hat{\mathbf{x}}^r = \left(\bar{\mathbf{\Phi}}^H\bar{\mathbf{\Phi}}\right)^{-1}\bar{\mathbf{\Phi}}^H\mathbf{y}$.
5. Calculate the signal magnitude and phase estimates by
$\rho_k = \left|\hat{\mathbf{x}}_k^{(r)}\right|, k = 1, \ldots, K$,
$\phi_k = \angle[\hat{\mathbf{x}}_k^{(r)}], k = 1, \ldots, K$.

where $\bar{N} \ll N$, $\mathbf{\Psi}$ represents the perturbed matrix caused by the grid bias, $\bar{\mathbf{x}}$ a new K-sparse vector of $\boldsymbol{\beta}$, $\mathbf{W}$ the diagonal weight matrix, and α is a trade-off parameter between sparsity and reconstruction accuracy, which can be selected properly via the L-curve method [28] or cross validation [29], [30].

By replacing $\mathbf{n}$ with $\mathbf{y} - \left(\bar{\mathbf{\Phi}} + \mathbf{\Psi}\right)\mathbf{x}$, the constrained SRE-STLS formulation in (24) can be equivalently transformed to the following unconstrained optimization problem:

$$\{\hat{\mathbf{x}}, \hat{\mathbf{\Psi}}\} = \arg\min_{\mathbf{x},\mathbf{\Psi}} \left[\left\|\mathbf{y} - \left(\bar{\mathbf{\Phi}} + \mathbf{\Psi}\right)\mathbf{x}\right\|_2^2 + \|\mathbf{\Psi}\|_F^2 + \alpha\|\mathbf{W}\mathbf{x}\|_1\right]. \tag{25}$$

The alternating descent algorithm is employed to obtain the refined multi-parameter estimation result. With available $\hat{\mathbf{x}}^{\mathfrak{p}}$ at the $\mathfrak{p}$-th iteration, $\mathbf{\Psi}$ can be estimated at the $(\mathfrak{p}+1)$-th iteration by solving the following convex problem

$$\hat{\mathbf{\Psi}}^{(\mathfrak{p}+1)} = \arg\min_{\mathbf{\Psi}} \left[\left\|\mathbf{y} - \left(\bar{\mathbf{\Phi}} + \mathbf{\Psi}\right)\hat{\mathbf{x}}^{(\mathfrak{p})}\right\|_2^2 + \|\mathbf{\Psi}\|_F^2\right] \tag{26}$$

whose closed form solution is

$$\hat{\mathbf{\Psi}}^{(\mathfrak{p}+1)} = (1 - \|\hat{\mathbf{x}}^{(\mathfrak{p})}\|_2^2)^{-1}[\mathbf{y} - \bar{\mathbf{\Phi}}\hat{\mathbf{x}}^{(\mathfrak{p})}](\hat{\mathbf{x}}^{(\mathfrak{p})})^T. \tag{27}$$

With obtained $\hat{\mathbf{\Psi}}^{(\mathfrak{p}+1)}$ and $\hat{\mathbf{x}}^{(\mathfrak{p})}$, the (b,b)-th element of weight matrix $\mathbf{W}^{(\mathfrak{p})}$ is first constructed as

$$\mathbf{W}_{b,b}^{(\mathfrak{p}+1)} = \frac{1}{|\hat{\mathbf{x}}_b^{(\mathfrak{p})}| + \varepsilon} \tag{28}$$

where the tuning parameter $\varepsilon > 0$ is used to provide stability and to ensure that a zero-valued component in $\hat{\mathbf{x}}^{(\mathfrak{p})}$ does not strictly prohibit a nonzero estimate at the next step [31]. The essence of applying the weight matrix $\mathbf{W}^{(\mathfrak{p})}$ is that large weights could be used to banish the entries whose indices are more likely to be outside of the signal support, which promotes sparsity at the right positions, finally reducing the penalization for larger coefficients and improving the recovery accuracy [32].

Next, $\hat{\mathbf{x}}^{(\mathfrak{p}+1)}$ is successively updated by solving the weighted LASSO-like optimization problem

$$\hat{\mathbf{x}}^{(\mathfrak{p}+1)} = \arg\min_{\mathbf{x}} \left[\left\|\mathbf{y} - (\bar{\mathbf{\Phi}} + \hat{\mathbf{\Psi}}^{(\mathfrak{p}+1)})\mathbf{x}\right\|_2^2 + \alpha\left\|\mathbf{W}^{(\mathfrak{p}+\mathbf{1})}\mathbf{x}\right\|_1\right] \tag{29}$$

and by finding indexes of the K largest peaks, DOA estimates and their corresponding refined small-scale OBM are further

Algorithm 3: SRE-STLS Based DOA and Magnitude-Phase Estimation

Input: Initial DOA estimates $\{\tilde{\theta}_1,\ldots,\tilde{\theta}_K\}$, array output $\mathbf{y}$, N_{max}, ε, τ, $\mathbf{\Psi}^{(1)}=\mathbf{0}_M$

Output: Refined DOA estimates $\{\tilde{\theta}_1^r,\ldots,\tilde{\theta}_K^r\}$, magnitude estimates $\{\tilde{\rho}_1,\ldots,\tilde{\rho}_K\}$ and phase estimates $\{\tilde{\phi}_1,\ldots,\tilde{\phi}_K\}$

1. Construct a small-scale OBM $\bar{\mathbf{\Phi}}$ around $\{\tilde{\theta}_1,\ldots,\tilde{\theta}_K\}$ with interval $\check{d}$.
2. **for** $\mathfrak{p}=1:N_{max}$

   Solve the general LASSO-like problem to yield the estimate of $\hat{\mathbf{x}}$:

   $$\hat{\mathbf{x}}^{(\mathfrak{p})}=\arg\min_{\mathbf{x}}\left[\left\|\mathbf{y}-(\bar{\mathbf{\Phi}}+\hat{\mathbf{\Psi}}^{(\mathfrak{p})})\mathbf{x}\right\|_2^2+\alpha\|\mathbf{x}\|_1\right]$$

   Update the estimation of perturbed matrix $\hat{\mathbf{\Psi}}^{(\mathfrak{p}+1)}$ through $\hat{\mathbf{\Psi}}^{(\mathfrak{p}+1)}=(1-\|\hat{\mathbf{x}}^{(\mathfrak{p})}\|_2^2)^{-1}[\mathbf{y}-\bar{\mathbf{\Phi}}\hat{\mathbf{x}}^{(\mathfrak{p})}](\hat{\mathbf{x}}^{(\mathfrak{p})})^T$.

   Construct the diagonal weight matrix $\mathbf{W}_{b,b}^{(\mathfrak{p}+1)}$ with its (b,b) element given by $\mathbf{W}_{b,b}^{(\mathfrak{p}+1)}=\frac{1}{|\hat{\mathbf{x}}_b^{(\mathfrak{p})}|+\varepsilon}$.

   Solve the weighted LASSO-like problem again with updated $\mathbf{W}_{b,b}^{(\mathfrak{p}+1)}$

   $$\hat{\mathbf{x}}^{(\mathfrak{p}+1)}=\arg\min_{\mathbf{x}}\left[\left\|\mathbf{y}-(\bar{\mathbf{\Phi}}+\hat{\mathbf{\Psi}}^{(\mathfrak{p})})\mathbf{x}\right\|_2^2+\alpha\left\|\mathbf{W}^{(\mathfrak{p}+1)}\mathbf{x}\right\|_1\right]$$

   to further obtain refined DOA estimates.

   $\check{d}\leftarrow\check{d}/2$, and refine $\bar{\mathbf{\Phi}}$ around improved DOAs with interval $\check{d}$.

   end
3. Output the final refined DOA estimates $\{\tilde{\theta}_1^r,\ldots,\tilde{\theta}_K^r\}$.
4. Construct another diagonal weight matrix $\mathbf{W}^{(\mathfrak{f})}$ as

   $$\mathbf{W}^{(\mathfrak{f})}=\mathrm{diag}\{I(\hat{\mathbf{x}}^{\mathfrak{f}},\tau)\}\text{ with }I(x,v)=\begin{cases}0, x>v\\ 1, x\le v.\end{cases}$$
5. Perform (27) and (29) after replacing $\bar{\mathbf{\Phi}}$ with $\bar{\mathbf{\Phi}}^{(\mathfrak{f})}$ and $\mathbf{W}^{(\mathfrak{f})}$ with $\mathbf{W}^{(\mathfrak{p}+1)}$ to obtain the final estimate $\hat{\mathbf{x}}^r$
6. Calculate the signal magnitude and phase estimates by

   $\rho_k=\left|\hat{\mathbf{x}}_k^{(r)}\right|, k=1,\ldots,K,$

   $\phi_k=\angle[\hat{\mathbf{x}}_k^{(r)}], k=1,\ldots,K.$

updated. Consequently, by performing steps (26)-(29) alternately, the final reconstruction result $\hat{\mathbf{x}}^{(\mathfrak{f})}$ and its corresponding DOA estimates and OBM $\bar{\mathbf{\Phi}}^{(\mathfrak{f})}$ at this stage are obtained.

Nevertheless, it is necessary to point out that the weight for nonzero coefficients in $\mathbf{x}$ is always nonzero, which implies that nonzero coefficients are still penalized, and such a property is indeed not beneficial for accurate magnitude-phase estimation. To avoid this issue, a further weighted LASSO-like optimization problem is constructed at the last step, whose weight matrix is constructed as

$$\mathbf{W}^{(\mathfrak{f})}=\mathrm{diag}\left\{I\left(\hat{\mathbf{x}}^{(\mathfrak{f})},\tau\right)\right\} \tag{30}$$

where τ is a user defined threshold and set to be the absolute value of the K-th largest non-zero element here, and $I(x,v)$ the indicator function, defined by

$$I(x,v)=\begin{cases}0, & x>v\\ 1, & x\le v.\end{cases} \tag{31}$$

Performing (27) and (29) after replacing $\bar{\mathbf{\Phi}}$ with $\bar{\mathbf{\Phi}}^{(\mathfrak{f})}$ and $\mathbf{W}^{(\mathfrak{f})}$ with $\mathbf{W}^{(\mathfrak{p}+1)}$, the unbiased reconstruction result $\hat{\mathbf{x}}^r$ and magnitude-phase estimation result of its nonzero elements are then achieved.

Proposition 1: For high SNRs or $\|\mathbf{n}\|_2\to 0$, the adopted SRE-STLS formulation will yield the following results:

$$\|\boldsymbol{\rho}-|\boldsymbol{\beta}|\|_2\to 0, \|\boldsymbol{\phi}-\angle[\boldsymbol{\beta}]\|_2\to 0 \tag{32}$$

where $\boldsymbol{\rho}=[\tilde{\rho}_1,\ldots,\tilde{\rho}_K]^T$ and $\boldsymbol{\phi}=[\tilde{\phi}_1,\ldots,\tilde{\phi}_K]^T$.

Proof: See the Appendix. ■

Remark 1: Proposition 1 indicates that the proposed solution can achieve improved and satisfactory magnitude-phase estimation, which will provide a fundamental condition for subsequent robust vehicle positioning. In detail, due to signal attenuation associated with the mobility characteristics of the vehicle, magnitude information cannot provide reliable and separable label features. However, it reflects the received SNR to some extent, which provides an important parameter for subsequent reliable DOA set selection. In contrast, phase information remains markedly more stable and thus offers a reliable feature for distinguishing different vehicles, which will be verified by subsequent simulations.

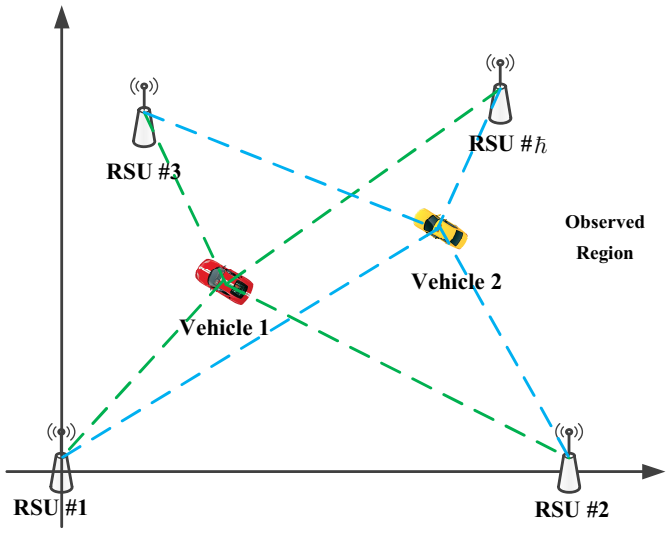

Fig. 3. Diagram for DOA based collaborative vehicle positioning.

Remark 2: In comparison with the general weight matrix in (28), the designed weight matrix in (30) will not penalize the K largest nonzero elements any more, guaranteeing effective incident signal magnitude-phase estimation, as shown later by simulations.

The proposed SRE-STLS based DOA and magnitude-phase estimation method is tabulated in Algorithm 3.

D. Collaborative Vehicle Positioning

As shown in Fig. 3, $\mathcal{L}$ RSUs are deployed at the positions of $\#\hbar\,(\lambda_{\hbar,x},\lambda_{\hbar,y})$, $\hbar=1,\ldots,\mathcal{L}$, and the coordinates of the k-th vehicle are assumed to be (x_k,y_k), whose corresponding DOAs with respect to RSUs are $\theta_{\hbar,k}$. In practice, once the DOAs of a certain vehicle are obtained, its corresponding coordinates can be derived via the cross-location principle easily. Taking two of the RSUs as an example, whose coordinates are assumed to be $\#1\,(0,0)$ and $\#2\,(\lambda_{2,x},0)$ for simplicity. Then, we have

$$x_k=\frac{\lambda_{2,x}\tan\theta_{2,k}}{\tan\theta_{1,k}+\tan\theta_{2,k}}, y_k=\frac{\lambda_{2,x}\tan\theta_{1,k}\tan\theta_{2,k}}{\tan\theta_{1,k}+\tan\theta_{2,k}}. \tag{33}$$

Nevertheless, there are normally multiple vehicles and more than two RSUs within the observed region in practice. Under such circumstances, two key issues need to be addressed. The first one is how to avoid the ambiguity problem among different vehicles, as the RSU cannot effectively distinguish which

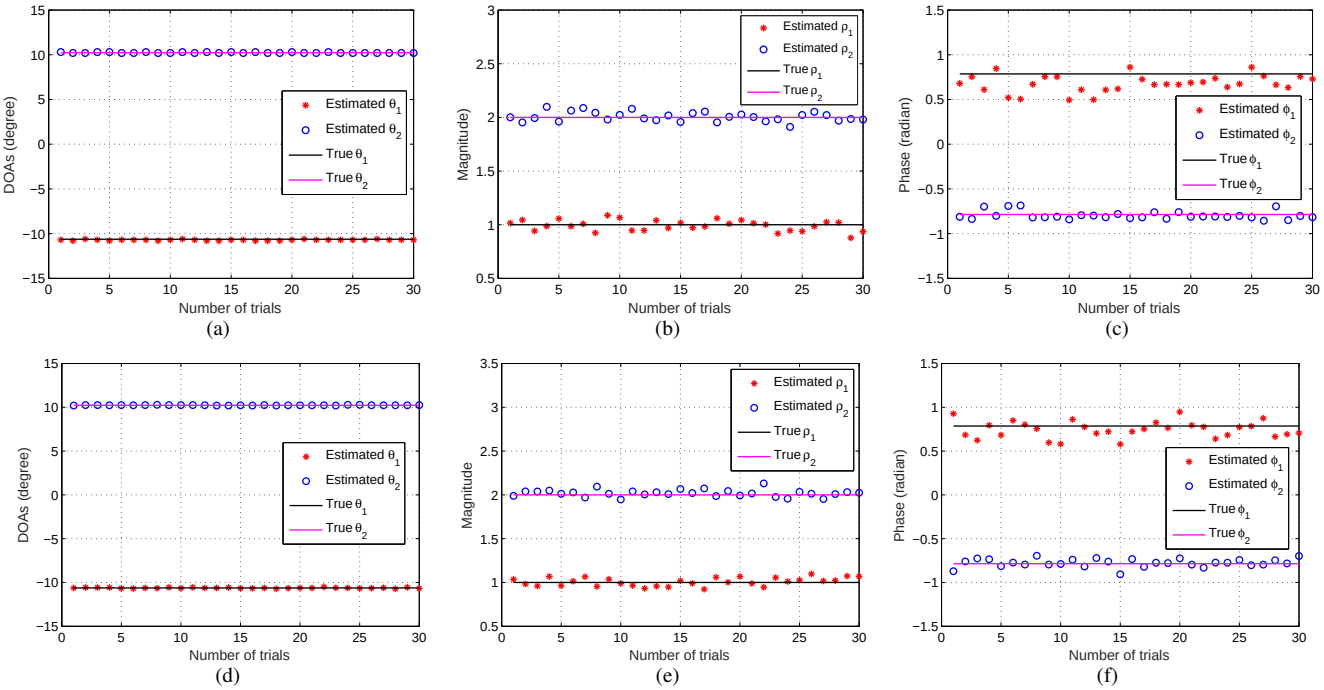

Fig. 4. Intuitive multi-parameter estimation result obtained by the proposed two algorithms with $M = 60$ and SNR=6 dB: (a)-(c) are the simulation results obtained by the proposed GAMP-LS algorithm, (d)-(f) are those by the proposed SRE-STLS algorithm.

DOA corresponds to which vehicle. The existing methods generally assume that they can be distinguished by default, but there is indeed no specific way, restricting their practical applications. Fortunately, the proposed solution can achieve phase estimation of impinging vehicle signals, which provides a possible simple solution to tackle this issue, as shown later by simulations.

Another key issue is how to select the best DOA sets for vehicle positioning in scenarios of more than two RSUs. The general operation is to take the average operation on the available coordinates [8], [12], [13]. However, as different RSUs provide different levels of DOA estimation accuracy, the simple averaging operation is not the optimal choice [5], [19]. In view of this, a weighted three-point cross-positioning method is introduced in [33], which first relies on the information of DOA estimates to construct the weights, and then exploit them to obtain enhanced vehicle positioning result. Such a method is a good attempt for robust vehicle positioning from DOA estimation perspective, but the main problem is that it relies solely on DOA information, which implies that there is still room for performance improvement.

The Cramér-Rao Bound (CRB) provides a theoretical lower bound for the unbiased DOA estimator, which is derived by considering all array configuration parameters. Its value reflects the overall DOA estimation performance from a global perspective. Compared to directly using a single array configuration parameter (such as received signal magnitude, incident DOA information, etc.) for reliable DOA selection, the CRB based criterion is more reasonable and universally applicable. Suppose that the noise level for all RSUs are the same. Inspired by the closed-form expression of CRB [34], [35], a principle to select the two most reliable DOA estimates for the k-th vehicle under a large-scale sensor array is developed as follows:

$$\{\theta_{\#1,k}, \theta_{\#2,k}\} = \arg\min_{\hbar} \left\{ \frac{1}{M_{\hbar}^3 \cos\theta_{\hbar,k}^2 \rho_{\hbar,k}} \right\} \tag{34}$$

where $\arg\min\{\cdot\}$ returns two DOAs that result in the smallest values within the curly brackets. In detail, the number of sensors $M_{\hbar}$ for each RSU is known a *priori*, and the impinging DOA $\theta_{\hbar,k}$ and signal magnitude $\rho_{\hbar,k}$ have also been estimated via the proposed methods in Sections III-A and III-B. Hence, $\theta_{\#1,k}$ and $\theta_{\#2,k}$ can be easily obtained. Different from existing state-of-the-art solutions, the adopted DOA set selection criterion fully considers the impact of various array configuration factors, which implies that $\theta_{\#1,k}$ and $\theta_{\#2,k}$ would be more reliable and reasonable than those obtained by other methods. As a result, an improved vehicle positioning result can be guaranteed, as verified later by simulations.

Remark 3: It is necessary to clarify that our solution is an alternative to GPS positioning, designed to provide the vehicle's absolute position information. Computer simulations show that the response time (single positioning time) of the GAMP-based locator is at the millisecond level, allowing the position update frequency (PUF) to reach from tens to hundreds of Hertz. With this frequency as the upper limit, the PUF can be flexibly adjusted based on the specific vehicle positioning scenario. For example, in lane-level accuracy-based V2I (Vehicle-to-Infrastructure) and V2V (Vehicle-to-Vehicle) safety applications, the PUF can be reduced to the required 10 Hz to balance accuracy requirements and computational load [36]. In coarse positioning applications with lower accuracy requirements, the PUF can be further reduced to 1 Hz [37], thereby achieving more efficient resource utilization. After obtaining the position information of vehicles, their velocity can be further estimated using the principle of time-

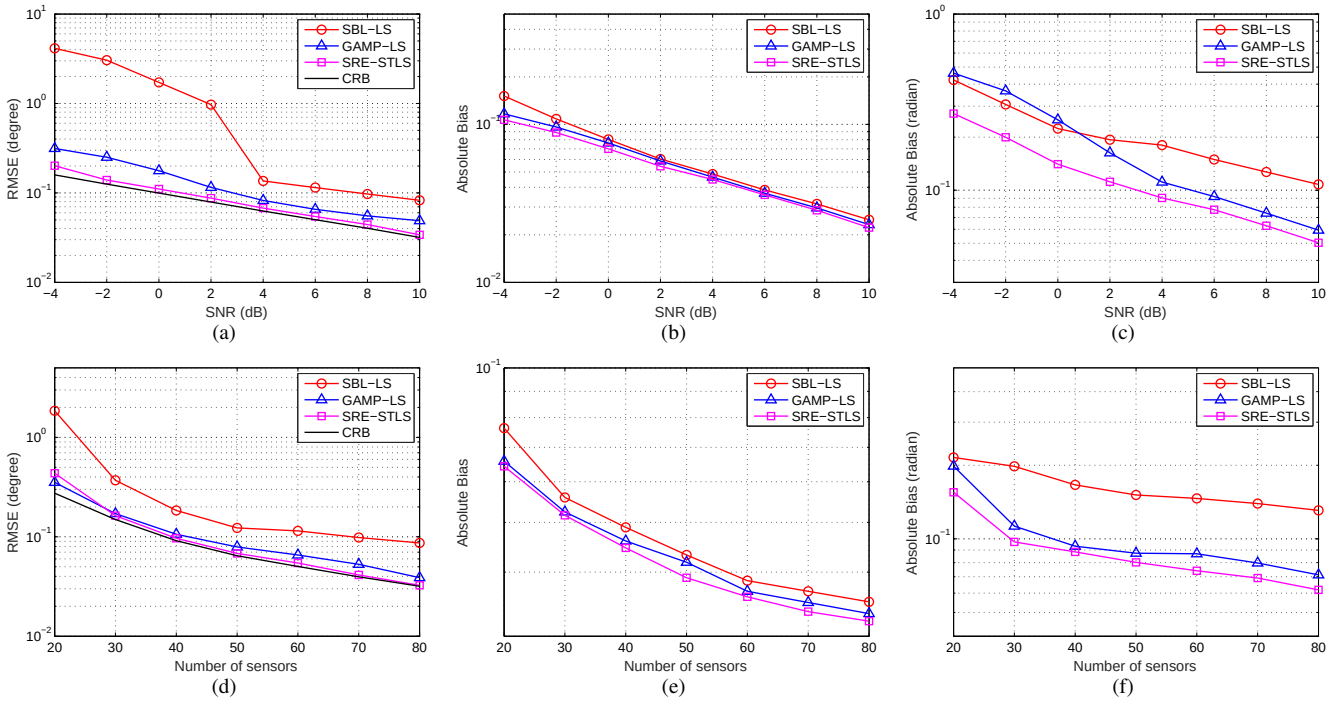

Fig. 5. Performance of multi-parameter estimation results under various array configurations: (a)-(c) are the RMSE of DOA estimation and AE of magnitude-phase estimation versus SNR with $M = 60$, respectively, (e)-(f) are those versus M with SNR=6 dB, respectively.

series data association [38],[39],[40]. With available velocity information, the PUF can be effectively reduced, leading to significant reduction in required computational resources. Suppose the vehicle positioning accuracy requirement in a certain application scenario is $d_{standard}$, and the maximum single positioning absolute error of the locator is ΔD with original PUF=$1/\mathcal{H}$. Then, the maximum velocity estimation deviation can be simply calculated by $\Delta v = 2\Delta D/\mathcal{H}$; as a result, the corresponding cumulative positioning error generated by Δv in the subsequent m_c response cycles becomes $2m_c\Delta D$. In this case, to meet the positioning accuracy requirements, it is necessary to satisfy $2m_c\Delta D \leq d_{standard}$. In other words, to guarantee the vehicle positioning accuracy of $d_{standard}$, $m_c \leq d_{standard}/2\Delta D$, and the re-positioning frequency can be reduced to $1/(m_c+1)$ of the original PUF[1].

E. Computational Complexity

Computational complexity is a key metric for vehicle positioning in practical applications. For the proposed methods, the major computational complexity comes from the first-stage GAMP-BP based initial DOA estimation and second-stage refined DOA and magnitude-phase estimation. The first-stage estimation only needs to calculate the product of the matrix and vector, whose corresponding complex multiplications are in the order of $\mathcal{O}(MN)$. For the proposed GAMP-LS algorithm, the required complexity at the second stage mainly comes from performing the inverse operation of $M \times \bar{N}$ OBM N_{max} times, which requires $\mathcal{O}(M\bar{N}^2 N_{\max})$; for the proposed SRE-STLS algorithm, the required complexity at the second stage mainly lies in the calculation of $\hat{\mathbf{\Psi}}$ and $\hat{\mathbf{x}}^{(r)}$ according to (27) and (29), which requires $\mathcal{O}\{(M\bar{N}+\bar{N}^3)(N_{max}+1)\}$ in total. Since $\bar{N} \ll N$ and $N_{max} = 2$ or 3 is enough as verified by numerical simulations, the final overall complexity of the proposed two solutions are roughly in the order of $\mathcal{O}(MN)$, which indicates that both methods are computationally efficient. Considering the estimation performance analysis above, the proposed solutions will be good candidates for practical vehicle positioning.

[1]As shown in the subsequent simulation, with 60 sensors and 6 dB SNR, the positioning accuracy of the proposed algorithm is below 0.1 m. In the lane-level positioning scenario, $d_{standard} = 1$ m [36], [37], implying that the re-positioning frequency can be reduced to at least $1/6$ of the original PUF.

IV. Simulations

In this section, the performance of the proposed solutions is examined via numerical simulations. The SBL combined with the designed LS (named as SBL-LS) algorithm in Section III-B and the CRB are included for comparison. In the simulations, the initial DOA estimates are obtained with a grid interval $\breve{d} = 0.1°$. For performance evaluation, the root mean square error (RMSE) for DOA estimation, the absolute error (AE) for magnitude-phase estimation and vehicle positioning, obtained from an average of 300 independent Monte-Carlo trials are employed, which are respectively defined as

$$\mathrm{RMSE}_\theta = \sqrt{\frac{1}{300K}\sum_{i=1}^{300}\sum_{k=1}^{K}\left(\hat{\theta}_{i,k}-\theta_k\right)^2} \quad (35)$$

$$\mathrm{AE}_\rho = \frac{1}{300K}\sum_{i=1}^{300}\sum_{k=1}^{K}\left|\hat{\rho}_{i,k}-\rho_k\right| \quad (36)$$

$$\mathrm{AE}_\phi = \frac{1}{300K}\sum_{i=1}^{300}\sum_{k=1}^{K}\left|\hat{\phi}_{i,k}-\phi_k\right| \quad (37)$$

$$\mathrm{AE}_p = \frac{1}{300K}\sum_{i=1}^{300}\sum_{k=1}^{K}\sqrt{\left(\hat{x}_{i,k}-x_k\right)^2+\left(\hat{y}_{i,k}-y_k\right)^2} \quad (38)$$

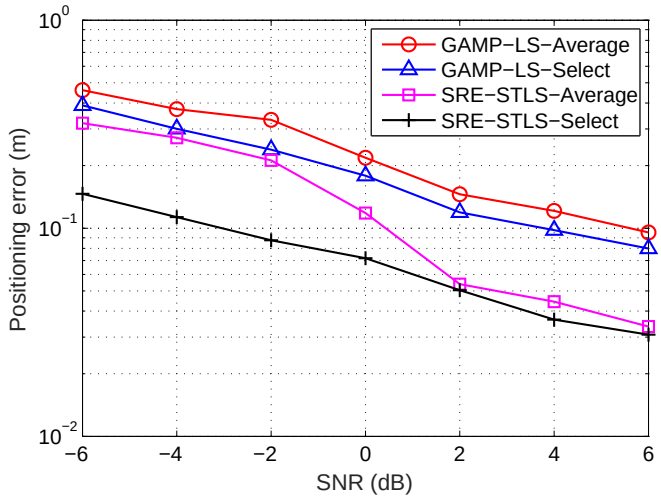

Fig. 6. Collaborative vehicle positioning performance for two vehicles versus the reference SNR under the deployment of three RSUs, each equipped with $M = 60$ sensors.

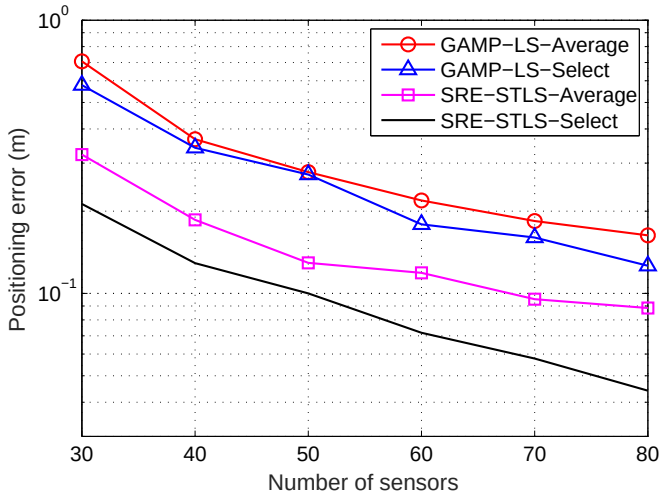

Fig. 7. Collaborative vehicle positioning performance for two vehicles versus the number of sensors M under the deployment of three RSUs, and the reference SNR is set to 0 dB.

where $\hat{\chi}_{i,k}$ denotes the estimate of χ_k in the ith trial.

In the first simulation, the multi-parameter estimation result obtained by the proposed GAMP-LS and SRE-STLS is provided in Fig. 4, where two incident signals are modeled as $\beta_1 = 1 \cdot e^{j\pi/4}$ and $\beta_1 = 2 \cdot e^{-j\pi/4}$ with their corresponding DOAs $\{\theta_1 = -10.625°, \theta_2 = 10.225°\}$; the number of sensors M and the received SNR are set to 60 and 6 dB, respectively. Figs. 4(a)-4(c) are the results provided by the GAMP-LS algorithm, while Figs. 4(d)-4(f) are those by the SRE-STLS algorithm. It can be observed that both proposed solutions can yield satisfactory and distinguished DOA and magnitude-phase estimation results, which not only validates the effectiveness of the proposed methods, but also provides a solid preliminary foundation for reliable vehicle positioning in subsequent stages.

In the second simulation, we further assess their performance with different SNRs and different number of sensors. The simulation result is shown in Fig. 5, where two source signals with magnitude one and phases $\phi_1 = \pi/4$ and $\phi_2 = -\pi/4$ are considered. In Figs. 5(a)-5(c), the number of sensors is fixed at 60, and SNR varies from -4 dB to 10 dB with a step of 2 dB. It can be seen that the performance of all algorithms improves with the increase of SNR, and both of the proposed algorithms outperforms the SBL-LS algorithm. In addition, the proposed SRE-STLS algorithm in DOA estimation even follows CRB very closely, showing its great superiority and robustness against noise. For signal phase estimation, although the proposed GAMP-LS underperforms the SBL-LS algorithm when SNR$\leq$ 0 dB, it performs better than the SBL-LS algorithm in relatively larger SNRs. In addition, the proposed SRE-STLS algorithm significantly performs better than the other algorithms in terms of phase estimation. In Figs. 5(d)-5(f), SNR is set to 6 dB, while the number of sensors M varies from 20 to 80 with a step of 10. From the simulation result, we can see that the two proposed solutions perform better than the SBL-LS algorithm again in the whole observed region, and the performance of the proposed SRE-STLS algorithm even surpasses all other algorithms.

In the last simulation, we further test the vehicle positioning performance of the proposed two algorithms. Three RSUs are deployed, and each RSU is equipped with an ULA composed of 60 sensors. The coordinates of three RSUs are $\#1\,(0m, 0m)$, $\#2\,(50m, 0m)$ and $\#3\,(0m, 50m)$, and the locations of two vehicles are $(25m, 20m)$ and $(30m, 40m)$, respectively. The received SNR (designated as SNR_1) at the RSU $\#1$ is taken as the reference, and those at other RSUs are defined as $\text{SNR}_\hbar = 10\lg\frac{d_1}{d_\hbar} + \text{SNR}_1$, where $d_\hbar$ denotes the distance between a certain vehicle and RSU $\#\hbar$, and the additive noise level at all RSUs are assumed to be the same. With all available DOAs, both the traditional average operation (with label 'Average') and the designed selection principle (with label 'Select') are employed for final vehicle positioning. The results are shown in Figs. 6 and 7, where M is set to 60, and SNR varies from -6 dB to 6 dB in Fig. 6; the reference SNR is set to 0 dB, and M varies from 30 to 80 in Fig. 7. It can be seen that the performance of the proposed SRE-STLS based vehicle positioning solution is better than that of GAMP-LS, which is similar with the conclusion in the second simulation. Moreover, it can be further observed that the proposed reliable DOA set selection principle can yield significantly improved positioning result, in comparison with the commonly adopted average operation, finally verifying the superiority of our proposed strategy. Particularly, by employing the reliable DOA set selection principle, the proposed SRE-STLS based solution can reach centimeter-level positioning accuracy in scenarios of SNR>-4 dB and $M \geq 50$, which provides a possible alternative tool for advanced levels of autonomous driving.

V. Conclusion

A novel vehicle positioning scheme jointly utilizing single-snapshot DOA and impinging signal magnitude-phase estimation is proposed in this paper. Different from existing state-

of-the-art pure DOA estimation methods, a two-stage strategy for estimating DOA and impinging signal magnitude-phase parameters is adopted, where the first stage is to obtain initial DOA estimation with the GAMP-BP algorithm, under the assumption of complex discrete random variable with distinct phase information, and the second step is to achieve improved DOA and magnitude-phase estimation with the GAMP-LS and SRE-STLS algorithms, respectively. Meanwhile, a more robust principle than the commonly used averaging operation for selecting reliable DOA sets is designed under multiple collaborative RSUs. Theoretical analysis and simulation results show that the proposed methods can not only yield satisfactory and computationally efficient multi-parameter estimation results, but also lead to an unambiguous and significantly improved positioning performance. In our future research, we will focus on how to achieve better DOA and signal feature estimation in multi-snapshot scenarios, as well as improved vehicle positioning results without ambiguity.

APPENDIX
PROOF OF PROPOSITION 1

Let $\xi = \max_{\bar{p},\bar{q}} |\mathrm{Re}\{\mathbf{G}(\bar{p},\bar{q})\}|$ denote the mutual coherence of $\bar{\mathbf{\Phi}}$ with $\mathbf{G} = \tilde{\mathbf{\Phi}}^H\tilde{\mathbf{\Phi}}$ and $\tilde{\mathbf{\Phi}} = \bar{\mathbf{\Phi}} + \mathbf{\Psi}$. Further assume that the number of vehicles/sources $K < 1/\xi + 1$ and $\|\mathbf{n}\|_2 \le \varepsilon \le \varsigma \to 0$. Then, according to the stable sparse recovery theory [41] and the analysis in [42], [43], [44], the LASSO and/or weighted LASSO estimators can lead to accurate estimation of DOA or indexes of nonzero elements even with perturbations present in both OBM $\bar{\mathbf{\Phi}}$ and $\mathbf{y}$. With such good DOA estimates, the perturbed matrix $\mathbf{\Psi}$ will be restricted to a small value, which can be further well estimated through formulation (26) due to its convexity.

With well estimated $\mathbf{\Psi}$ (represented by $\hat{\mathbf{\Psi}}^{(\mathfrak{f})}$), formulation (29) with $\overline{\mathbf{\Phi}}^{(\mathfrak{f})}$ and $\mathbf{W}^{(\mathfrak{f})}$ can be equivalently transformed into the following constrained optimization problem

$$\hat{\mathbf{x}}^{(r)} = \min \|\mathbf{W}^{(\mathfrak{f})}\mathbf{x}\|_1 \; s.\,t.\; \mathbf{y} - (\overline{\mathbf{\Phi}}^{(\mathfrak{f})} + \hat{\mathbf{\Psi}}^{(\mathfrak{f})})\mathbf{x}_2^2 \le \varsigma \quad (39)$$

where ς is a new penalized parameter related to α.

If $\hat{\mathbf{x}}^{(r)}$ is the minimizer of $\|\mathbf{W}\mathbf{x}\|_1$, it can be derived that

$$\|\mathbf{W}^{(\mathfrak{f})}\hat{\mathbf{x}}^{(r)}\|_1 \le \|\mathbf{W}^{(\mathfrak{f})}\mathbf{x}\|_1. \quad (40)$$

Subsequently, if DOA or nonzero indexes of $\mathbf{x}$ are estimated accurately and threshold parameter τ is selected properly, it will yield that

$$\left\|\mathbf{W}^{(\mathfrak{f})}\mathbf{x}\right\|_1 = 0,\; \sum\nolimits_{l\in\zeta} |\mathbf{x}_l| = 0 \quad (41)$$

where ζ denotes the support of zeros in $\mathbf{x}$ and ζ^c its corresponding complement.

As a result, the reconstruction error will be bounded by

$$\left\{ \begin{array}{l} \sum_{l\in\zeta} |\boldsymbol{\nu}_l| = 0, \#\zeta^c \le K \\ (1+\xi)\|\boldsymbol{\nu}\|_2^2 - \xi\|\boldsymbol{\nu}\|_1^2 \le (\varepsilon+\varsigma)^2 \end{array} \right\} \quad (42)$$

where $\boldsymbol{\nu} = \mathbf{x} - \hat{\mathbf{x}}^{(r)}$ and $\boldsymbol{\nu}_l$ represents its l-th element.

Notice that $\sum_{l\in\zeta} |\mathbf{x}_l| = 0$, and we then have $\|\nu\|_1^2 \le K\|\nu\|_2^2$, which directly yields

$$(1+\xi)\|\boldsymbol{\nu}\|_2^2 - \xi K\|\boldsymbol{\nu}\|_2^2 \le (\varepsilon+\varsigma)^2. \quad (43)$$

Finally, it can be obtained that

$$\|\boldsymbol{\nu}\|_2^2 \le \frac{(\varepsilon+\varsigma)^2}{1+\xi(1-K)} \to 0 \quad (44)$$

which further implies

$$\|\boldsymbol{\rho} - |\boldsymbol{\beta}|\|_2 \to 0, \|\boldsymbol{\phi} - \angle[\boldsymbol{\beta}]\|_2 \to 0. \quad (45)$$

This concludes the proof of proposition 1.

REFERENCES

[1] Y. Gao, H. Jing, M. Dianati, C. M. Hancock and X. Meng, "Performance analysis of robust cooperative positioning based on GPS/UWB integration for connected autonomous vehicles," *IEEE Trans. Intell. Veh.*, vol. 8, no. 1, pp. 790-802, Jan. 2023.

[2] P. McLaughlin and C. Vagg, "A new method of vehicle positioning using bumps and road surface defects," *IEEE Trans. Intell. Transp. Syst.*, vol. 23, no. 8, pp. 13655-13665, Aug. 2022.

[3] X. Li, Y. Tan, Z. Shen, X. Li, and Y. Zhou, "GNSS-based cooperative instantaneous precise positioning aided by multi-epoch and multi-agent associations," *IEEE Trans. Veh. Technol.*, vol. 73, no. 6, pp. 7771-7784, Jun. 2024.

[4] A. Boukerche, H. Oliveira, E. Nakamura, and A. Loureiro, "Vehicular ad hoc networks: A new challenge for localization-based systems," *Comput. Commun.*, vol. 31, no. 12, pp. 2838-2849, Jul. 2008.

[5] H. Xu, M. Jin, and Q. Guo, "Vehicle positioning with unitary approximate message passing-based DOA estimation under exact spatial geometry," *IEEE Internet Things J.*, vol. 11, no. 8, pp. 14938-14948, Apr. 2024.

[6] X. Lu, Z. Wei, R. Xu, L. Wang, B. Lu, and J. Piao, "Integrated sensing and communication enabled multiple base stations cooperative UAV detection," in *Proc. 2024 IEEE Int. Conf. Commun. Workshops (ICC Workshops)*, Denver, CO, USA, 2024, pp. 1882-1887.

[7] Y. Li, F. Shu, B. Shi, X. Cheng, Y. Song, and J. Wang, "Enhanced RSS based UAV localization via trajectory and multi-base stations," *IEEE Commun. Lett.*, vol. 25, no. 6, pp. 1881-1885, Jun. 2021.

[8] S. Zhao, X.-P. Zhang, X. Cui, and M. Lu, "Optimal two-way TOA localization and synchronization for moving user devices with clock drift," *IEEE Trans. Veh. Technol.*, vol. 70, no. 8, pp. 7778-7789, Aug. 2021.

[9] M. Martal`, S. Perri, G. Verdano, F. De Mola, F. Monica, and G. Ferrari, "Improved UWB TDoA-based positioning using a single hotspot for industrial IoT applications," *IEEE Trans. Ind. Inform.*, vol. 18, no. 6, pp. 3915-3925, Jun. 2022.

[10] X. Wang, L. T. Yang, D. Meng, M. Dong, K. Ota, and H. Wang, "Multi-UAV cooperative localization for marine targets based on weighted subspace fitting in SAGIN environment," *IEEE Internet Things J.*, vol. 9, no. 8, pp. 5708-5718, Apr. 2022.

[11] M. Xu, *et al.*, "CFAR based NOMP for linear spectral estimation and detection," *IEEE Trans. Aerosp. Electron. Syst.*, vol. 59, no. 5, pp. 6971-6990, Oct. 2023.

[12] F. Wen, J. Wang, J. Shi, and G. Gui, "Auxiliary vehicle positioning based on robust DOA estimation with unknown mutual coupling," *IEEE Internet Things J.*, vol. 7, no. 6, pp. 5521-5532, Jun. 2020.

[13] M. Chen, R. Zeng, Z. Zhang, and H. Wang, "Multiple-RIS-aided vibrio foraging optimization positioning algorithm under internet of vehicles environment," *IEEE Trans. Intell. Veh.*, vol. 9, no. 1, pp. 2390-2398, Jan. 2024.

[14] H. Xu, W. Liu, M. Jin, and Y. Tian, "Positioning and contour extraction of autonomous vehicles based on enhanced DOA estimation by large-scale arrays," *IEEE Internet Things J.*, vol. 10, no. 13, pp. 11792-11803, Jul. 2023.

[15] L. Han, *et al.*, "Two-dimensional multi-snapshot newtonized orthogonal matching pursuit for DOA estimation," *Digital Signal Process.*, vol. 121, pp. 103313, 2022.

[16] H. Wang, L. Wan, M. Dong, K. Ota, and X. Wang, "Assistant vehicle localization based on three collaborative base stations via SBL-based robust DOA estimation," *IEEE Internet Things J.*, vol. 6, no. 3, pp. 5766-5777, Jun. 2019.

[17] H. Wang, X. Wang, X. Lan, T. Su, and L. Wan, "BSBL-based auxiliary vehicle position analysis in smart city using distributed MEC and UAV-deployed IoT, *IEEE Internet Things J.*, vol. 10, no. 2, pp. 975-986, 15 Jan.15, 2023.

[18] L. Wan, Y. Sun, L. Sun, Z. Ning, and J. J. P. C. Rodrigues, "Deep learning based autonomous vehicle super resolution DOA estimation for safety driving," *IEEE Trans. Intell. Transp. Syst.*, vol. 22, no. 7, pp. 4301-4315, Jul. 2021.

[19] Y. Tian, S. Liu, W. Liu, H. Chen, and Z. Dong, "Vehicle positioning with deep-learning-based direction-of-arrival estimation of incoherently distributed sources," *IEEE Internet Things J.*, vol. 9, no. 20, pp. 20083-20095, Oct. 2022.
[20] S. Rangan, "Generalized approximate message passing for estimation with random linear mixing," in *IEEE Int. Symp. Inf. Theory Proc.*, St. Petersburg, Russia, Jul. 2011, pp. 2168-2172.
[21] X. Zhang, K. Huo, S. Zhang, Y. Liu, W. Jiang, and X. Li, "Low-complexity optimization for direction-of-arrival estimation via approximate message passing," in *27th European Signal Process. Conf. (EUSIPCO)*, A Coruna, Spain, Nov. 2019, pp. 1-5.
[22] F. R. Kschischang, B. J. Frey, and H. A. Loeliger, "Factor graphs and the sum-product algorithm," *IEEE Trans. Infor.Theory*, vol. 47, no. 2, pp. 498-519, Feb. 2001.
[23] J. Pearl, *Probabilistic reasoning in intelligent systems: networks of plausible inference.*, SanMateo, CA, USA: MorganKaufmann, 2014.
[24] Z. Meng, D. Wei, A. Wiesel, and A. O. Hero, "Marginal likelihoods for distributed parameter estimation of Gaussian graphical models," *IEEE Trans. Signal Process.*, vol. 62, no. 20, pp. 5425-5438, Oct. 2014.
[25] R. Tibshirani, Regression selection and shrinkage via the lasso, *J. Roy. Stat. Soc. B*, vol. 58, no. 1, pp. 267-288, 1996.
[26] X. Xu, X. Wei, and Z. Ye, "DOA estimation based on sparse signal recovery utilizing weighted ℓ_1-norm penalty," *IEEE Signal Process. Lett.*, vol. 19, no. 3, pp. 155-158, Mar. 2012.
[27] Y. Tian, X. Sun, and S. Zhao, "DOA and power estimation using a sparse representation of second-order statistics vector and ℓ_0-norm approximation," *Signal Process.*, vol. 105, pp. 98-108, May 2014.
[28] P. C. Hansen, "Analysis of discrete ill-posed problems by means of the L-curve," *SIAM Rev.*, vol. 34, no. 4, pp. 561-580, 1992.
[29] P. Boufounos, M. F. Duarte, and R. G. Baraniuk, "Sparse signal reconstruction from noisy compressive measurements using cross validation," in *Proc. IEEE Workshop Statist. Signal Process.*, Madison, WI, USA, Aug. 2007, pp. 299-303.
[30] R. Ward, "Compressed sensing with cross validation," *IEEE Trans. Inf. Theory*, vol. 55, no. 12, pp. 5773-5782, Dec. 2009.
[31] L. He, H. Wu, X. Wen, and J. You, "Seismic acoustic impedance inversion using reweighted L1-norm sparse constraint," *IEEE Geosci. Remote Sens. Lett.*, vol. 19, pp. 1-5, Apr. 2022.
[32] C. Zheng, G. Li, H. Zhang, and X. Wang, "An approach of DOA estimation using noise subspace weighted ℓ_1 minimization," in *Proc. IEEE Int. Conf. Acoust., Speech Signal Process. (ICASSP)*, Prague, Czech Republic, 2011, pp. 2856-2859.
[33] D. Meng, X. Li, and W. Wang, "Robust sparse recovery based vehicles location estimation in intelligent transportation system," *IEEE Trans. Intell. Transp. Syst.*, vol. 25, no. 1, pp. 1023-1032, Jan. 2024.
[34] M. Pesavento and A. Gershman, "Maximum-likelihood direction-of arrival estimation in the presence of unknown nonuniform noise," *IEEE Trans. Signal Process.*, vol. 49, no. 7, pp. 1310-1324, Jul. 2001.
[35] A. J. Weiss and B. Friedlander, "DOA and steering vector estimation using a partly calibrated array," *IEEE Trans. Aerosp. Electron. Syst.*, vol. 32, no. 3, pp. 1047-1057, Jul. 1996.
[36] N. Williams and M. Barth, "A qualitative analysis of vehicle positioning requirements for connected vehicle applications," *IEEE Intell. Transp. Syst. Mag.*, vol. 13, no. 1, pp. 225-242, Spring 2021.
[37] [Online]. Available: http://local.iteris.com/cvria/html/applications/applic-ations.html.
[38] G. Liu, "On velocity estimation using position measurements," in *Proc. 2002 American Control Conf. (IEEE Cat. No.CH37301)*, Anchorage, USA, 2002, pp. 1115-1120.
[39] R. H. Brown, S. C. Schneider, and M. G. Mulligan, "Analysis of algorithms for velocity estimation from discrete position versus time data," *IEEE Trans. Ind. Electron.*, vol. 39, no. 1, pp. 11-19, Feb. 1992.
[40] F. Janabi-Sharifi, V. Hayward and C. . -S. J. Chen, "Discrete-time adaptive windowing for velocity estimation," *IEEE Trans. Control Syst. Technol.*, vol. 8, no. 6, pp. 1003-1009, Nov. 2000.
[41] C. Zhu, "Stable recovery of sparse signals via regularized minimization," *IEEE Trans. Inf. Theory.*, vol. 54, no. 7, pp. 3364-3367, Jul. 2008.
[42] E. J. Candes, M. B. Wakin, and S. P. Boyd, "Enhancing sparsity by reweighted ℓ_1 minimization, *J. Fourier Anal. Appl.*, vol. 14, nos. 5-6, pp. 877-905, Dec. 2008.
[43] H. Zhu, G. Leus, and G. B. Giannakis, "Sparsity-cognizant total least-squares for perturbed compressive sampling," *IEEE Trans. Signal Process.*, vol. 59, no. 5, pp. 2002-2016, May 2011.
[44] Y. Tian, H. Yue, and X. Rong, "Multi-parameters estimation of coherently distributed sources under coexistence of circular and noncircular signals," *IEEE Commun. Lett.*, vol. 24, no. 6, pp. 1254-1257, Jun, 2020.

Ye Tian (Member, IEEE) received the B.S. and Ph.D. degrees from the College of Communication Engineering, Jilin University, Changchun, China, in 2009 and 2014, respectively. He won a Huawei scholarship in 2013 and was selected as a young top talent by the Hebei Provincial Department of Education in 2016. He is currently an Associate Professor in Faculty of Information Science and Engineering, Ningbo University. He has published 50+ journal and conference papers and 10+ patents. His research interests include array signal processing, autonomous vehicle positioning, massive MIMO as well as large-dimensional random matrix theory.

Shiqi Shu received the B. Eng. degree from Hunan Institute of Science and Technology, Yueyang, China, in 2022. He is currently working toward M.S. degree in Communication Engineering with the Faculty of Electrical Engineering and Computer Science in Ningbo University. His research focuses on sensor array signal processing, approximate message passing, and direction-of-arrival estimation.

Wei Liu (Senior Member, IEEE) received his BSc (Space Physics) and LLB (Intellectual Property Law) degrees from Peking University, China, in 1996 and 1997, respectively, MPhil from the Department of Electrical and Electronic Engineering, University of Hong Kong in 2001, and PhD from the School of Electronics and Computer Science, University of Southampton, UK, in 2003. He then worked as a postdoc first at Southampton and later at Imperial College London. From 2005 to 2023, he was a Lecturer/Senior Lecturer at the Department of Electronic and Electrical Engineering, University of Sheffield, UK and from 2023 to 2024, a Reader at the School of Electronic Engineering and Computer Science, Queen Mary University of London. Since 2024, he has been a Professor at the Department of Electrical and Electronic Engineering, Hong Kong Polytechnic University. He has published 430+ journal and conference papers, six book chapters, and two research monographs titled "Wideband Beamforming: Concepts and Techniques" (Wiley, 2010) and "Low-Cost Smart Antennas" (Wiley, 2019), respectively. His research interests cover a wide range of topics in signal processing, with a focus on sensor array signal processing and its various applications, such as robotics and autonomous systems, human computer interface, radar, sonar, and wireless communications.

He is a member of the Applied Signal Processing Systems Technical Committee (2023-2025) of the IEEE Signal Processing Society (SPS), the Digital Signal Processing Technical Committee of the IEEE Circuits and Systems Society (Chair for 2022-2024), and the IEEE SPS Education Board (2024-2026, Chair of its Educational Conference Program Committee), and a former member of the Sensor Array and Multichannel Signal Processing Technical Committee of the IEEE SPS (Chair for 2021-2022), the IEEE SPS Technical Directions Board (2021-2022), and the IEEE SPS Conference Board and its Executive Subcommittee (2022-2023). He also acted as an associate editor for IEEE Trans. on Signal Processing, IEEE Access, and Journal of the Franklin Institute, and currently he is an associate editor for IEEE Antennas and Wireless Propagation Letters, and an Executive Associate Editor-in-Chief of the Frontiers of Information Technology and Electronic Engineering. He is an IEEE Distinguished Lecturer for the Aerospace and Electronic Systems Society (2023-2024).

He Xu received the B.E. and M.E. degrees from the College of Communication Engineering, Jilin University, Changchun, China, in 2010 and 2013, respectively, and Ph.D. degree from the Faculty of Information Science and Engineering, Ningbo University in 2024. From 2014 to 2020, she worked as a Research Assistant in Yanshan University. Since 2024, she has been a lecturer at the School of Cyber Science and Engineering, Ningbo University of Technology, China. Her main research interests include direction-of-arrival estimation, target positioning, massive MIMO, integrated sensing and communication.

Hua Chen (Senior Member, IEEE) received the M.Eng. degree and Ph.D. degree in Information and Communication Engineering from Tianjin University, Tianjin, China, in 2013 and 2017, respectively. From Apr. 2025, he is a one-year visiting scholar at the Department of Electrical and Electronics Engineering, Nanyang Technological University, Singapore. He is now as an Associate Professor in Faculty of Electrical Engineering and Computer Science, Ningbo University, China. His research interests include array signal processing, MIMO radar and RIS-aided Localization. He is currently an Associate Editor for IEEE Signal Processing Letters and Circuits, Systems, and Signal Processing.